Applied Energy 352 (2023) 121933

Contents lists available at ScienceDirect

Applied Energy

journal homepage: www.elsevier.com/locate/apenergy

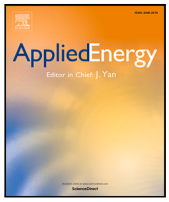

Heat pump integration in non-continuous industrial processes by Dynamic Pinch Analysis Targeting

Jasper V.M. Walden [a,*], Beat Wellig [b], Panagiotis Stathopoulos [a]

[a] German Aerospace Center (DLR), Institute of Low-Carbon Industrial Processes, Simulation and Virtual Design, Walther-Pauer-Straße 5, Cottbus, 03046, Brandenburg, Germany

[b] Lucerne University of Applied Sciences and Arts, Competence Center Thermal Energy Systems and Process Engineering, Technikumstrasse 21, Horw, 6048, Switzerland

ARTICLE INFO

Keywords:
Process integration
Pinch analysis
Industrial heat pump
Non-continuous processes
Mathematical programming

ABSTRACT

A key strategy for the transition towards a low-carbon economy is the electrification of industrial heat. Heat pumps can recover and upgrade excess or waste heat. They present a highly efficient component to decarbonize process heating. In Pinch Analysis, most approaches to design the heat recovery system as well as the utility system are based on a single operating point or a couple of operating point. In the past, this was due to the lack of temporally detailed process data. However, the available process data is expected to increase drastically by the use of transient process simulation models. Thus, a method is needed which interprets the data correctly and assists with design choices.

This study proposes a methodology for the design and sizing of a heat pump based on the simulated annual process data of an industrial process. Three approaches are explored: (1) the conventional approach for heat pump integration by application of the Time Average Model (TAM), (2) an approach that investigates the optimal heat pump parameters for each data point by the principles of Pinch Analysis and mathematical optimization and (3) an optimization method, which considers the entire annual process data as well as thermo-economic objectives such as net present value (NPV) and internal rate of return (IRR).

The new methodology compared to the conventional TAM approach is able to design a 33 % smaller heat pump, which reduces the annual operating cost by an additional 2.2 %. The NPV and IRR are more than tripled.

1. Introduction

Decarbonizing the industry is a crucial step towards mitigating the effects of anthropogenic climate change, as industrial processes contribute significantly to global greenhouse gas emissions [1]. The majority of the energy in industrial processes is demanded in the form of heat [2]. Consequently, heat usage as well as heat supply are essential to lower the greenhouse gas emissions. The overall systematic optimization of heat in industrial processes has been developed by Linnhoff and Flower [3]. The methodology is commonly referred to as Pinch Analysis.

1.1. State of the art

The development of Pinch Analysis presents a milestone in the systematic analysis of thermodynamic requirements within industrial processes. There have been a large number of contributions to the methodology within the past 40 years [4,5]. In reality, many industrial processes involve dynamic behaviour, such as start-up, shut-down, changes in production rate, batch processes and multi-product processes. The application of Pinch Analysis to non-continuous processes has been thoroughly developed based on the first works of Linnhoff [6]. Common approaches are the time-slice model (TSM) and the time-average model (TAM). The TAM averages the heat loads over the batch period and allows for basic targeting. The TSM divides the process into

* Corresponding author.
E-mail address: jasper.walden@dlr.de (J.V.M. Walden).

https://doi.org/10.1016/j.apenergy.2023.121933
Received 3 July 2023; Received in revised form 22 August 2023; Accepted 6 September 2023

Nomenclature

Acronyms

CAPEX	Capital expenditure
COP	Coefficient of performance
CU	Cold utility
DLR	German Aerospace Center
GCC	Grand Composite Curve
HO-HP	Hourly-optimized heat pump
HP	Heat pump
HU	Hot utility
IEA	International Energy Agency
IRR	Internal rate of return
NPV	Net present value
OPEX	Operational expenditure
R	Cash flow
TAM	Time average model
TO-HP	Temporally-optimized heat pump
TSM	Time slice model

Latin symbols

$\bar{p}$	Optimization variables
$\dot{Q}$	Heat flow rate
E	Cost function exponent
f	Cost function factor
m	Degression exponent
c	Cost
Q	Heat
T	Temperature
s	Operational cost savings

Greek symbols

$\alpha, \beta, \gamma, \zeta$	Function coefficients
η	Efficiency

Subscripts

boiler	Boiler
carnot	Carnot
coverage	Heat coverage by heat pump
el	Electricity
fuel	Fuel
Lang	Lang factor
lifetime	Lifetime
lift	Lift
om	Operating and maintenance
PI	Planning and installation
sink	Heat sink side of the heat pump
source	Heat source side of the heat pump
sys	System integration and peripherals

discrete time intervals based on the process schedule. These models are specifically suitable for cyclic production. Several studies [7,8] included variations in process streams and renewable energy sources by applying the time slice model. The challenges of heat integration in a non-continuous milk powder process have been investigated by Atkins et al. [9]. Eiholzer et al. [10] investigated the integration of solar energy into a brewery process by application of the TAM.

Apart from providing an approach on how to optimize the heat recovery system, the methodology offers a thermodynamic viewpoint on the correct integration and placement of a heat pump within an industrial process [11]. By application of the methodology a large variety of heat pump integration studies have been carried out. Becker et al. [12] investigated two different integration strategies for the integration of a heat pump in a cheese factory. The integration of a hybrid compression–absorption heat pump for convective dryers was investigated by Walmsley et al. [13]. Schlosser et al. [14] reviewed the integration of vapour-compression heat pumps for various industries and processes based on the Grand Composite Curve (GCC). The work by Wallerand et al. [15] demonstrated the optimal heat pump integration by mathematical optimization of the heat pump features. Additionally, some heat pump integration studies deal with non-continuous processes. Such as Stampfli et al. [16], who investigated the integration of a heat pump storage system into a non-continuous process by a hybrid method based on the insights of Pinch Analysis and mathematical optimization. Furthermore, Agner et al. [17] proposed a practical workflow for heat pump integration in non-continuous processes based on the Indirect Source Sink Profiles (ISSP). In the study conducted by Seevers et al. [18], the dimensioning of a heat pump storage system was demonstrated using a production line as a case study. The work by Becker et al. [19] presented a MILP method for targeting heat recovery and heat pump integration in multi-period problems. Most of the research on non-continuous processes is based on the TAM or the TSM. These models have been sufficient because commonly there is a lack of temporally resolved process data. However, there is no approximation of the induced error in design by the use of the TSM for scarce process data.

To tackle the scarcity of existing process data, several studies have combined simulation models and Pinch Analysis [20,21]. The term Dynamic Pinch Analysis has also been used for the application of Pinch Analysis to integrate ventilation waste heat in a greenhouse by Ghaderi et al. [22]. Furthermore, the work by Hosseinnia [23] points in a similar direction by conducting hourly energy targeting in buildings. Precise process simulations are increasingly prevalent and are capable to generate large datasets of process data. Additionally, the continuous integration of renewable energy sources in industrial processes will further amplify the need to have time-dependent process data to account for the availability of the energy sources during the operation of the system. Besides, the full knowledge of the process data can suggest different system designs in comparison to a scarce dataset. The work by Lal et al. [24] showed the impact of fluctuating process streams on the selection of the heat exchanger network.

Nevertheless, existing literature lacks a methodology for heat pump integration, which combines thermodynamic insights from Pinch Analysis and incorporates highly resolved simulated process data to propose optimal process integration strategies.

1.2. Research objective

The present study compares three different approaches for selecting the most economic parameters of a heat pump based on the annual process data. The three approaches include: (1) a conventional heat pump integration based on the TAM, (2) a statistical approach of calculating the optimal heat pump parameters for every process state and (3) an overall mathematical optimization, which considers all process states as well as thermo-economic objectives such as the net present value (NPV) and the internal rate of return (IRR). The following research questions are addressed:

- How do current heat pump integration methods change with the increasing knowledge about process data?
- How can the economically-optimal and thermodynamically feasible heat pump integration be determined for a large dataset of process data?
- What are the main parameters that significantly impact and constrain the performance of industrial heat pumps?

2. Methods

This section provides a detailed description of the conventional stationary heat pump integration, along with an overview of the three examined approaches for integrating a heat pump into a highly time-resolved and non-continuous simulated industrial process. The schematic representation of the approaches is depicted in Fig. 3.

2.1. Conventional heat pump integration

Townsend and Linnhoff [11] derived a methodology for the correct placement of energy conversion units such as heat engines and heat pumps. They formulated the Appropriate Placement Principle based on the GCC. The GCC is a visual representation of the net heat flow requirement at any given temperature after the implementation of all heat recovery measures. The Pinch Temperature represents the point where there is no net heat flow requirement, dividing the heat cascade into cooling and heating regions. Only by positioning the heat sink of the heat pump above the Pinch Temperature and the heat source below it, system improvement can be achieved. The heat pump integration can be determined and visualized by use of the GCC as shown in Fig. 1(a). T_{sink} describes the condenser temperature and $\dot{Q}_{\text{sink}}$ the emitted heat flow of the heat pump. Conversely, T_{source} is the temperature in the evaporator and $\dot{Q}_{\text{source}}$ the absorbed heat flow.

Mechanically driven heat pumps consume electricity to supply heat, which is generally more costly than fossil fuels, thus they must compensate for the extra operational expenses (OPEX) through their efficiency to ensure economic viability. According to Schlosser et al. [14], a Coefficient Of Performance (COP) greater than the ratio of electricity to reference fuel cost is required for economic feasibility:

$$COP_{real} > \frac{c_{\text{el}}}{c_{\text{fuel}}/\eta_{\text{boiler}}}. \tag{1}$$

The maximum achievable temperature lift of the heat pump is automatically constrained by the price ratio of electricity to reference fuel, as it directly influences the COP. As shown in Fig. 2 and described by Eq. (4), a higher temperature lift leads to a decrease in COP and an increase in the delivered heat $\dot{Q}_{\text{sink}}$ by the heat pump. This relationship is derived by combining Eq. (2) and the first part of Eq. (3). Therefore, the temperature lift represents a trade-off between the heat flow rate covered by the heat pump and its performance. While Eq. (1) provides a lower limit for the COP, it does not indicate the optimal COP.

$$\dot{Q}_{\text{sink}} = \dot{Q}_{\text{source}} + P_{\text{HP}} \tag{2}$$

$$\text{COP} = \frac{\dot{Q}_{\text{sink}}}{P_{\text{HP}}} = \eta_{\text{carnot}} \frac{T_{\text{sink}}}{T_{\text{sink}} - T_{\text{source}}} \tag{3}$$

$$\dot{Q}_{\text{sink}} = \frac{\text{COP} \cdot \dot{Q}_{\text{source}}}{\text{COP} - 1} \tag{4}$$

2.2. Investigated approaches

In this study, three distinct methodologies are assessed and contrasted to ascertain the most favourable parameters and dimensions for integrating a heat pump into the specified industrial process. The investigated approaches are designed to accommodate the dynamic heat requirements of the process and consider the economic constraints and considerations associated with the integration.

Mathematical optimization is employed to find the optimal balance between temperature lift and the heat flow rate covered by the heat pump. This optimization process is common to all three approaches. The subsequent section outlines the formulation of the optimization, followed by a description of the three distinct approaches for dynamic heat pump integration.

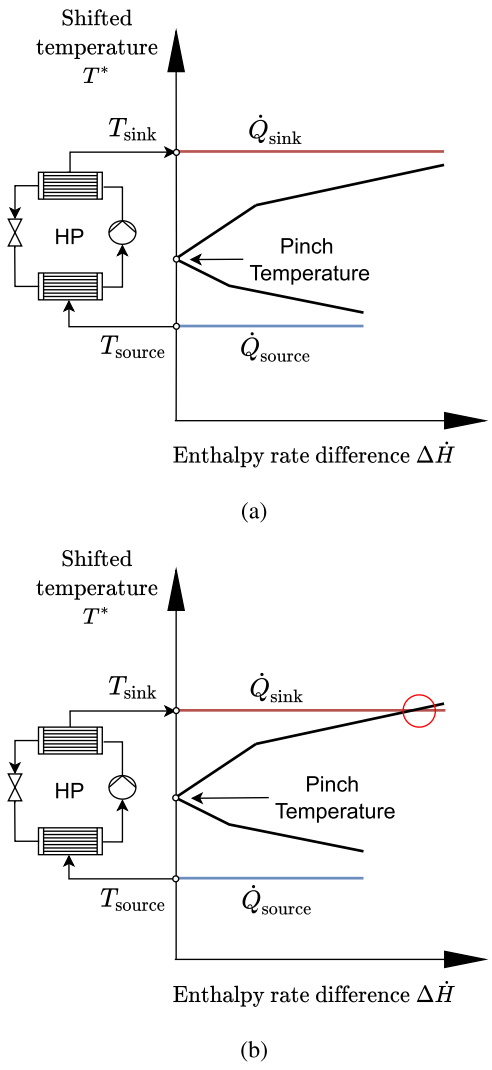

Fig. 1. Visualization of heat pump integration by Pinch Analysis. a) demonstrates the correct integration across the Pinch Temperature. b) shows a incorrect integration that is violating the heat sink constraint defined by the optimization problem formulated in Section 2.2.1.

2.2.1. Modelling and optimization

All of the three approaches use a similar optimization formulation. The optimization problem is shown in Eq. (5)–(8). The objective is to minimize the operating cost (OPEX). However, the objective of the temporally-optimized heat pump (TO-HP) is the summed annual OPEX, because the TO-HP approach allows to factor in the time dimension. Furthermore, the TO-HP optimization has been expanded to include total cost as the objective value. This is not possible for the TAM HP and the hourly-optimized heat pumps (HO-HPs), because the dimension of time is averaged or not considerable, respectively.

The source & sink temperatures of the heat pump and the heat pumps source heating capacity are the optimization variables (6). Constraints of the optimization are the temperature-dependent heat flow rates demanded by the process' GCC. The heat pumps heat source cannot uptake more heat than the currently available cooling demand by the process (8). Analogous for the heat flow rate of the heat sink (7). A violation of the heat sink constraint (7) is depicted in Fig. 1(b). The Figure illustrates that the heat pump's supplied heat flow rate surpasses the process demand at the heat sink temperature of the heat pump. The energy balance will be closed, however, this is a second law

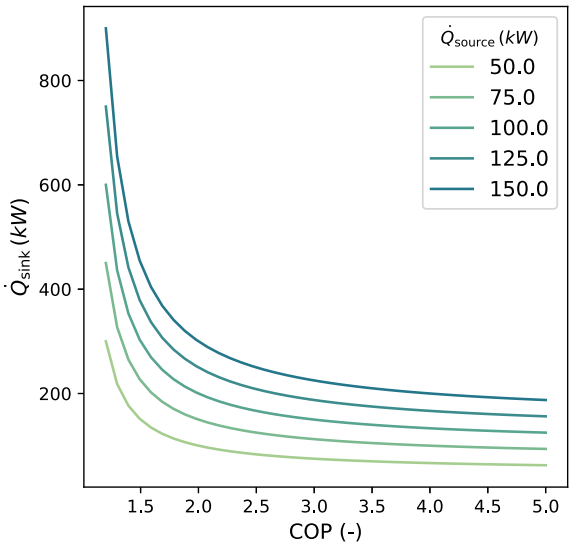

Fig. 2. The connection between the heat sink heat flow rate and the COP of a heat pump with constant heat source heat flow rate.

violation, since there is a temperature crossover and the process heat demand cannot be fulfilled by the heat pump. Consequently, there will be a hot utility demand, while the heat pump is producing excess heat, which introduces a cooling requirement. This case is infeasible and thus constrained in the optimization problem.

$$\min_{\bar{p}} \quad \left(c_{HU}\dot{Q}_{HU} + c_{CU}\dot{Q}_{CU} + c_{el}P_{HP}\right) \tag{5}$$

$$\bar{p} = [T_{source}, T_{sink}, \dot{Q}_{source}] \tag{6}$$

$$\text{s. t.} \quad \dot{Q}_{sink} \leq \dot{Q}_{h,GCC} \tag{7}$$

$$\dot{Q}_{source} \leq \dot{Q}_{c,GCC} \tag{8}$$

The heat load of the heat sink is calculated by Eq. (4).

Furthermore, the heat pump model is based on a regression model, because it provides a higher precision than conventional Carnot heat pump models [25]. Eq. (9) and the regression parameters (a = 1.9118, b = 0.044189, c = −0.89094, d = 0.67895) are taken from [25].

$$\text{COP} = a \cdot (T_{lift} + 2b)^c \cdot (T_{sink} + b)^d \tag{9}$$

The optimization problem's bounds are provided in Table 1, while the specific energy prices can be found in Table 2. Additionally, Table 4 presents the parameters for the heat pump cost functions. The parameters are identical for all three approaches. It should be noted that the upper bounds for the sink temperature and the heat flow rate of the heat pump are deliberately chosen to be large to keep the solutions less constrained. However, for the heat source temperature, the lower bound was set to 10 °C due to the fact, that if the cooling demand by the process drops below 10 °C it is preferable for the heat pump to use an ambient heat source. Also, in the case study no subzero temperatures are demanded by the process, consequently the cold utility (CU) should be able to cover this temperature region. The cost of CU c_{CU} is significantly lower because within the temperature range, where CU is required, cheap CU such as river water or cooling towers can be used.

The price ratio between electricity c_{el} and hot utility (HU) c_{HU} is selected to be 2, which should favour the integration of heat pumps with a COP higher than 2 as described in Eq. (1).

The temperature difference $\Delta T_{min,hp}$ between the heat pumps' streams and the GCC is calculated similarly as described by Stampfli et al. [16]. The heat pump is commonly connected to the process by a heat recovery loop (HRL). A ΔT_{HEX} is required between the process stream and the heat recovery loop. Furthermore, the latent heat transfer between the heat exchangers of the heat pump to the HRL requires a smaller temperature difference of $^3/_4\,\Delta T_{HEX}$, because of the higher heat transfer coefficient. In the GCC, the process streams are already shifted by $^1/_2\,\Delta T_{HEX}$. This adds up to a remaining temperature difference of $^5/_4\,\Delta T_{HEX}$. ΔT_{HEX} is chosen to be 5 K. Consequently, $\Delta T_{min,hp}$ is equivalent to 6.25 K.

Table 1
The bounds of the optimization variables.

	Value
T_{source} (°C)	[10, 40]
T_{sink} (°C)	[40, 250]
$\dot{Q}_{source}$ (kW)	[0, 5000]

Table 2
Parameters for the economic evaluation.

	Value
c_{HU}	80 (€/MWh)
c_{CU}	40 (€/MWh)
c_{el}	160 (€/MWh)
$n_{lifetime}$	20 (y)
i	7 (%)

The optimization is implemented in Python utilizing the SciPy optimization library [26]. The problem is solved with a differential evolution algorithm [27]. The definition for the heat pump heat coverage is given by (10).

$$Q_{coverage} = \frac{\int_0^t \dot{Q}_{sink}\,d\tau}{\int_0^t \dot{Q}_{HU}\,d\tau} \cdot 100 \tag{10}$$

2.2.2. Optimized TAM HP integration

The TAM averages the process stream data over the investigated period. The mathematical optimization procedure, described in Section 2.2.1, is applied to the TAM GCC and results in heat pump parameters, which are optimal based on the given TAM GCC.

Consequently, the heat pump is evaluated along all 8759 GCCs. Each GCC corresponds to a time slice of an hour, thus representing a year of 8759 h. By evaluating the entire year, the amount of operating hours in which the heat pump is operable can be calculated according to the chosen feasibility criterion. Furthermore, the total yearly heat demand, the percentage of the heat that is covered by the heat pump, the residual cost and total OPEX are calculated.

The feasibility criterion used in this study is based on the GCC. The optimized heat pump is evaluated for each of the 8759 GCCs. The heat pump is rendered as infeasible, if the heat pumps heat sink heat flow rate is exceeding the GCC at the heat sink temperature. Analogous, the heat pump is considered infeasible for the GCC or time-slice, if the heat source heat flow rate exceeds the GCC at the heat source temperature.

For each GCC, where the heat pump is feasible, the OPEX are calculated based on the electricity consumption of the heat pump and the residual HU & CU, that has to be supplied. The OPEX parameters can be found in Table 2. Furthermore, whenever the heat pump is considered feasible, it is added to the count of operating hours. Part-load of the heat pump, with a shift in thermal output or operating temperatures, is not considered in the scope of this work. If the heat pump is infeasible, the OPEX are solely based on the heating and cooling demand which has to be covered by utility.

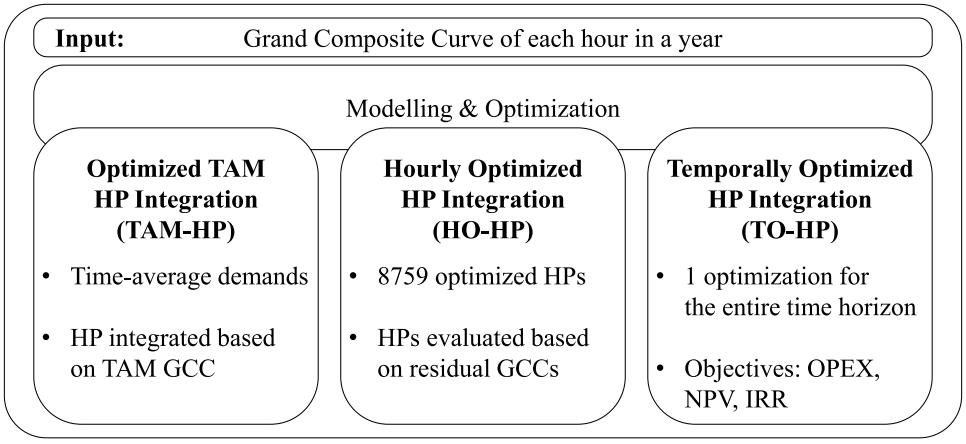

Fig. 3. Overview of the three investigated approaches for the heat pump integration.

2.2.3. Hourly optimized HP integration (HO-HP)

This approach is similar to the optimized TAM HP integration except that for each GCC the optimal heat pump parameters are determined. However, some GCCs do not have a region below the Pinch Temperature or the placed heat pump would exceed the bounds, thus no heat pump can be placed. For each hour one heat pump is created, which is then evaluated for each existing GCCs. The evaluation of the heat pump is analogous to the previously described TAM HP evaluation including the same feasibility criterion. The OPEX for each heat pump is determined by summing the resulting OPEX based on each evaluated GCC.

Without full knowledge of all time slices, one would measure process data for one or a couple of points in time and place a heat pump accordingly. However, by analysing all heat pumps for all time-slices, a trend of the heat pump parameters can be derived. Thus, the amount of cases in which i.e. the heat pump source temperature is chosen to be a certain value can be quantified. Through this approach, it is imperative to analyse whether the frequently occurring values also serve as optimal selections for heat pump parameters. Additionally, the distribution of heat pump parameters also serves as context for the other two approaches.

2.2.4. Temporally optimized HP integration (TO-HP)

As a logical consequence of the hourly-statistical approach, the third approach calculates an optimal set of heat pump parameters by mathematical optimization for all time slices. Additionally, three different objectives are investigated. One objective of the optimization is to minimize the summed OPEX over the whole year (11) to create a comparable case with the TAM HP and the HO-HPs.

$$\min_{\vec{p}} \quad \int_0^t \left(c_{\mathrm{HU}} \dot{Q}_{\mathrm{HU}} + c_{\mathrm{CU}} \dot{Q}_{\mathrm{CU}} + c_{\mathrm{el}} P_{\mathrm{HP}} \right) d\tau \tag{11}$$

The second objective, Eq. (12), is to maximize the NPV of the heat pump investment [28,29]. This objective also respects the CAPEX that are associated with the integration of a heat pump. The CAPEX increase with the size of the heat pump. Thus, this objective includes a trade-off for the dimension of the chosen heat pump.

$$\max_{\vec{p}} \quad \mathrm{NPV} = \sum_{x=0}^{N} \frac{R_x}{(1+i)^x} \tag{12}$$

The third objective (13) is to maximize the internal rate of return (IRR) of the heat pump investment. Although these metrics are closely connected, there are some distinct differences.

Maximizing the NPV returns the investment with the highest absolute value based on the lifetime. On the other hand, by maximizing the IRR, the investment with the highest rate of return will be chosen. Which means, the investment that returns a positive NPV in the quickest possible way, which can result in a different investment or in this case, a different heat pump.

$$\max_{\vec{p}} \quad \mathrm{IRR} \tag{13}$$

$$\text{with} \quad 0 = \sum_{x=0}^{N} \frac{R_x}{(1+\mathrm{IRR})^x} \tag{14}$$

The interest rate i is chosen to be 7% and the economic lifetime N to be 20 years. The cash flows R are assumed to be constant. The initial CAPEX are described in Section 2.3. The cash inflows of the investment are the annual savings s in OPEX by using a heat pump instead of fulfilling the entire heat demand with utility (15).

$$\mathrm{s} = c_{\mathrm{opex,no\ hp}} - c_{\mathrm{opex,hp}} \tag{15}$$

2.3. Industrial heat pump cost functions

Several different approaches to estimate the cost of process equipment or entire units can be found in the literature [30]. Commonly models such as the Lang factor method [31] or modifications of the six-tenths rule [32] are utilized. Furthermore, regression models of existing installations and devices are used [33]. Some works estimate the total unit cost of a heat pump by its component costs [16,34]. Fig. 4 compares different specific heat pump cost functions. The cost functions and their references can be found in Table 3, while their parameters are listed in Table 4. It should be noted, that Table 3 presents the total cost functions, however, Fig. 4 shows the specific cost.

The compared functions consist of a function for large-scale heat pumps by Schlosser et al. [35], a Lang factor cost function [31], a regression on large-scale district heating heat pumps with flue-gas as heat source by Pieper et al. [33], the cost projection of the European Commission [36] and cases which have been documented in the IEA Annex 35 [37].

A key similarity between all compared functions is the decreasing specific unit cost with increasing installed heat pump capacity. This effect is associated with the economies of scale. The greatest differences in cost estimations are below 500 kW_{th} of installed heat sink capacity. The cost function of Schlosser et al. makes a distinction at 210 kW_{th} which increases the steepness of specific cost for units with heat capacity below 210 kW_{th}. The authors modified the cost function by Schlosser et al. slightly by addition of an operation and maintenance factor, which is estimated to be 1% of the CAPEX.

The present work calculates the CAPEX of the heat pump with the correlation provided by Schlosser et al. [35]. Nevertheless, it should be stated that every cost function comes with great uncertainty and is often strongly dependent on the site-specific conditions.

Table 3
Functions for the investment cost of large-scale heat pumps.

Name	Function	Reference
Schlosser et al.	$f_{HP} \cdot \dot{Q}_{sink}^{E_{HP}} \cdot f_{PI} \cdot f_{sys} \cdot f_{om}$	[35]
Pieper et al.	$\alpha \cdot \dot{Q}_{sink} + \beta$	[33]
Lang factor	$c_{base} \cdot \left(\frac{\dot{Q}_{sink}}{\dot{Q}_{ref}}\right)^{m} \cdot f_{Lang}$	[31]
European Commission	$\gamma \cdot \dot{Q}_{sink}^{\zeta}$	[36]

Table 4
Parameters of the heat pump cost functions presented in Table 3.

Schlosser et al.	[35]
f_{HP}	$\begin{cases} 1521\,(e/kW_{th}) & \text{if } \dot{Q}_{sink} \le 210\,kW_{th} \\ 349.5\,(e/kW_{th}) & \text{if } \dot{Q}_{sink} > 210\,kW_{th} \end{cases}$
E_{HP}	$\begin{cases} 0.637 & \text{if } \dot{Q}_{sink} \le 210\,kW_{th} \\ 0.912 & \text{if } \dot{Q}_{sink} > 210\,kW_{th} \end{cases}$
f_{pi}	1.25 (–)
f_{sys}	1.8 (–)
f_{om}	1.01 (–)
Pieper et al.	[33]
α	0.43686 (M€/MW)
β	0.094874 (M€)
Lang factor method	[31]
c_{base}	50,000 (€)
$\dot{Q}_{ref}$	100 (kW)
f_{Lang}	3 (–)
m	0.42 (–)
European Commission	[36]
γ	0.352 (M€/MW)
ζ	−0.122 (–)

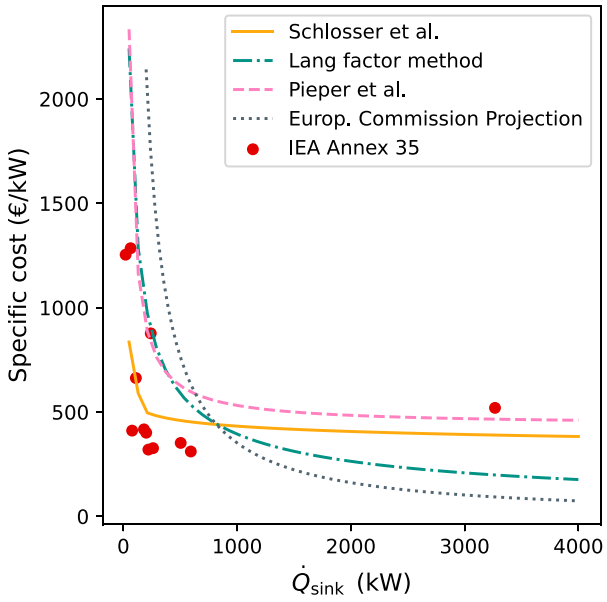

Fig. 4. Comparison of specific cost functions for large-scale heat pump installations.

3. Case study

This study utilizes a transient simulation dataset of an automotive paint shop, similar to the work conducted by Giampieri et al. [38]. The analysis assumes that the process operates on an hourly basis throughout the entire year, with the simulated process data encompassing all 8759 h. The variations in heating and cooling demands primarily arise from weather conditions. The aim of this paper is to outline and compare different approaches to solve dynamic heat pump integration, the specifics of the underlying process are not addressed in this work.

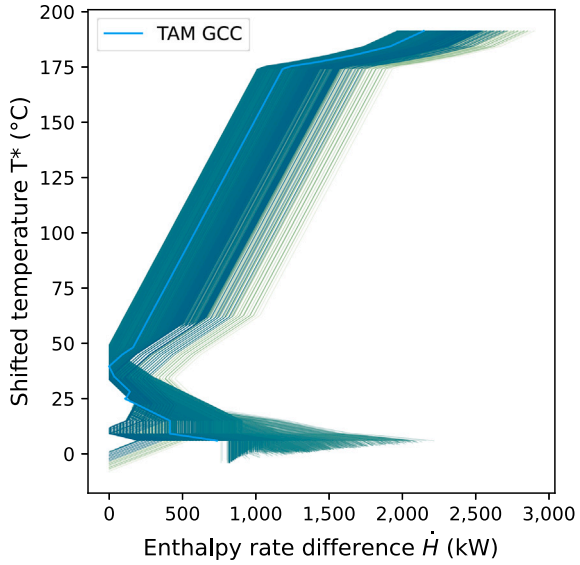

Fig. 5. Visualization of the Grand Composite Curves throughout the 8759 process states.

The basis of the present work are 8759 GCCs, which are presented in Fig. 5. The GCC based on the TAM is also visualized. Each of the GCCs represents an individual operating point.

A heat pump placement, according to the appropriate placement principle and the bounds described in Table 1, is feasible in 7574 h, which amounts to 86.5% of all investigated GCCs.

4. Results

The investigated approaches are put into relation to each other. A histogram in Fig. 6 presents insights about the occurrence of parameters of the hourly optimized heat pumps. Count refers to the number of cases in each bin. So in this case, the number of cases of a certain value indicated on the horizontal axis.

The expectation was, that the most frequently chosen values for the optimization parameters are optimal. However, in Fig. 6a) it can be seen, that the most common heat source temperature is approximately 16 °C. Similarly, the TAM HP resulted at 15 °C temperature as source temperature. The source and sink temperatures of the temporally-optimized heat pumps (TO-HPs) are slightly higher. The TAM HP is in the region of the most frequently chosen values except for the sink temperature. However, the TO-HPs, which are optimized with knowledge over the entire year, have different heat pump dimensions. The heat sink and heat source capacities of the TO-HPs are similar as most frequent chosen hourly-optimized HPs (HO-HPs). Additionally, the TO-HPs heat sink temperatures are intermediate in comparison to the HO-HPs, while the COPs are again aligning with the most frequently chosen COP by the HO-HPs. Fig. 6d) shows that for the most operating points, a heat pump with a COP of 2.5 is optimal. The OPEX and NPV TO-HPs show a similar COP, however, with different source and sink temperatures. By changing the heat pumps temperatures more operating hours and a greater heat coverage by the heat pump is accomplished, which results in a lower annual OPEX as it will be shown in the following.

The COP value is expected to be bigger than 2 in any case, since the price ratio of HU and electricity was chosen to be 2. The COP has to make up for the higher cost of electricity, which the heat pump consumes to provide a more economical case (see Eq. (1)).

It should be noted, that the TO-HP, with the objective to maximize the IRR, selects a significantly smaller heat pump with a greater COP. This increases the return of the investment, due to a lower initial investment required for a smaller heat pump. Fig. 7 presents the source

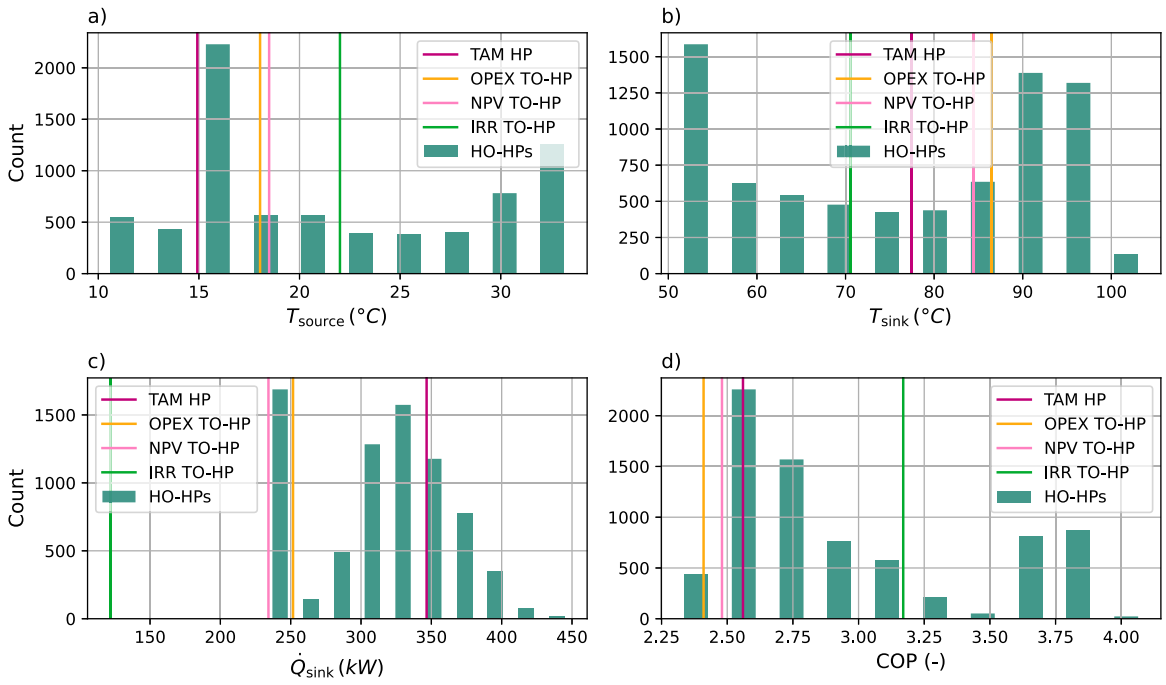

Fig. 6. Histogram of the hourly-optimized heat pump results, with coloured vertical lines representing the optimized parameters obtained through the integration approaches.

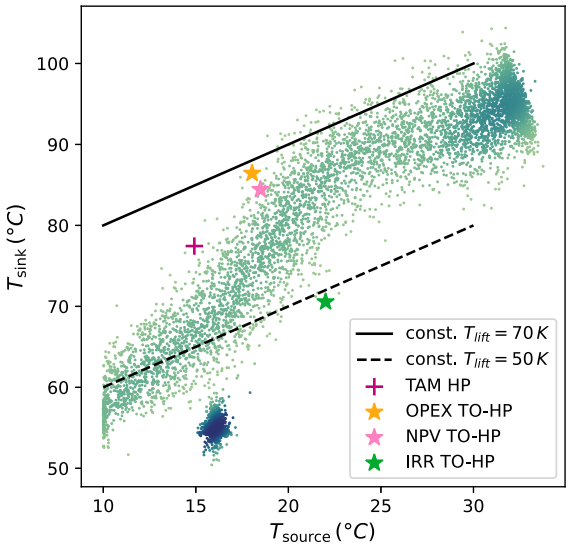

Fig. 7. The HP heat source and heat sink temperatures by integration approach. The scattered distribution represents the hourly-optimized heat pumps for each time step, with darker colours indicating higher density.

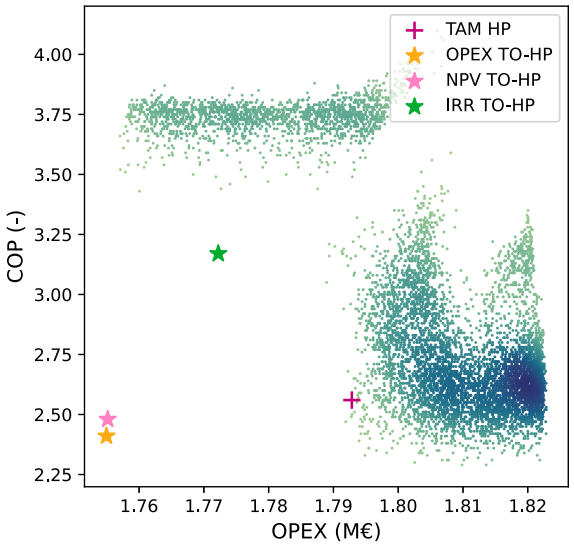

Fig. 8. Coefficient of performance of the heat pumps in relation to the annual operating expenditures.

and sink temperatures of the three approaches. At a T_{source} of 15 °C the density of points is increased strongly, which is indicated by a darker colour. The black lines in Fig. 7 show that the majority of the heat pumps have a temperature lift between 50 K and 70 K, which includes the TO-HPs.

Fig. 8 shows that COPs of 3.6 and higher are optimal for some GCCs, but overall a higher temperature lift and lower COP is preferable with the objective to reduce the total annual OPEX. Commonly, heat pumps with a high COP would be considered more economical, but the higher temperature lift of the TO-HPs leads to the heat pump being feasible in more operating points and thus, it can operate during more hours in the year (see Fig. 9). As a result, the summed OPEX of the entire year is lower. Furthermore, the TAM HP provides a fairly economical fit in terms of annual OPEX, which is unexpected, since the TAM GCC was calculated solely on the basis of the mean values of each process stream. A larger COP does not imply lower OPEX when considering an entire year.

In Fig. 9, the proportion of the total annual heat demand fulfilled by the heat pump is plotted against the operating hours of each heat pump. The definition of the heat pump coverage can be found in Eq. (10). Logically, if the heat pump covers more operating hours, its annual heat coverage is increasing likewise. Thus, a linear correlation between the increase in operating hours and the amount of heat coverage provided by the heat pump is observed. Furthermore, the NPV & OPEX TO-HP are feasible in more operating points and thus, their economic performance is beneficial. A similar finding has been made in [39], in which the levelized cost of heat of a heat pump is reduced by more operating hours.

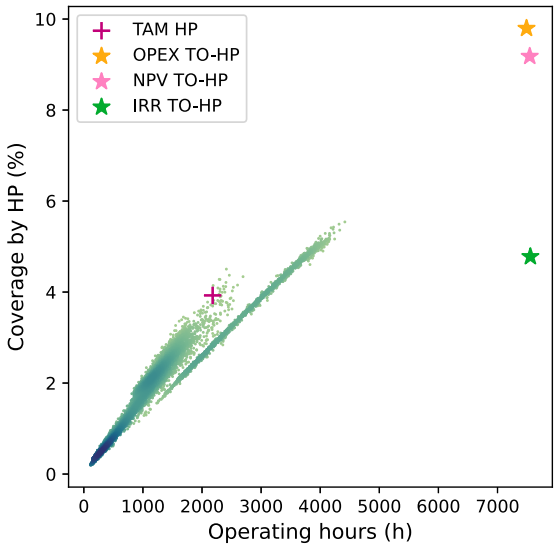

Fig. 9. The annual feasible operating hours and the total amount of heat demand covered by each heat pump. The definition of the heat coverage can be found in Eq. (10).

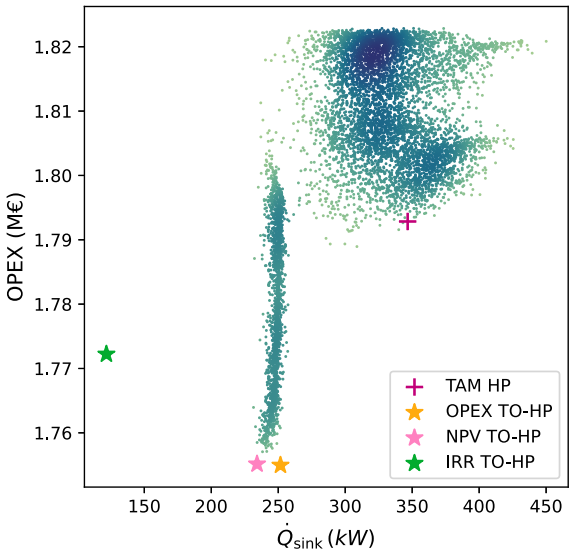

Fig. 10. The total annual operating cost in relation to the installed heating capacity of each heat pump.

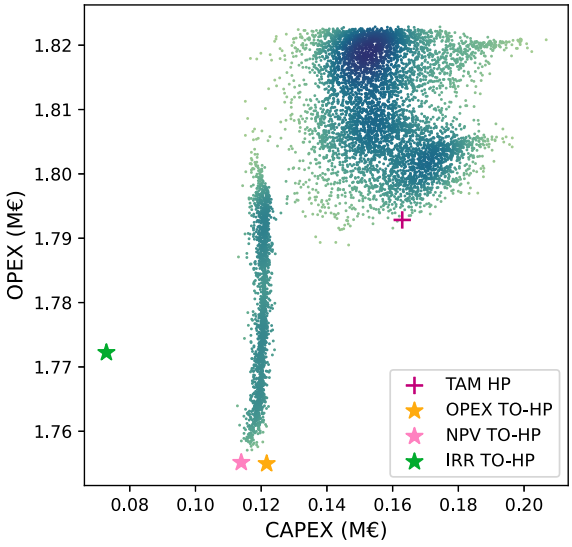

Fig. 11. The economic trade off between operating expenditures and capital expenditures.

The heat pump, that is optimized for a maximized IRR presents an outlier. As previously stated, it operates on different source and sink temperatures with a lower temperature lift and higher COP. The optimization found a combination, which is feasible in 7556 h. However, it is still able to provide 4.78% of the annual heat demand.

The heat coverages of the optimized heat pumps of approximately 4.7%–10% are low. This is partly due to the selected feasibility criterion. The operating points in which the heat pump is operable, strongly depend on the previously described feasibility criterion (Section 2.2.2). A heat pump with a heating capacity greater than the current heat demand is rendered infeasible. However, if the heating capacity is smaller than the current demand, the heat pump is feasible. In other words, the investigated heat pumps do not have a part-load capability and only design points are considered. This generally favours smaller heat pumps. Consequently, the heat coverage is low even though the operating hours are high, because of the small heating capacity of the heat pumps. Additionally, the steepness of the GCCs, as presented in Fig. 5, does not favour large phase change heat pumps. Because a greater heating capacity requires a larger temperature lift, which in turn decreases the COP. Generally, for steep GCCs transcritical or sensible heat pumps are beneficial, because the temperature glide can be matched by the heat pump.

Fig. 10 shows why the IRR TO-HP provides a lower coverage with equally high operating hours — its heat sink is significantly smaller. Essentially, the IRR TO-HP is a smaller heat pump with a higher COP. Which results in higher annual OPEX compared to larger heat pumps as the NPV and OPEX TO-HPs, because of the smaller heat coverage. In comparison, the HO-HPs are designed with greater heat sink dimensions, albeit with higher annual OPEX. This is mostly due to their low feasibility and consequently low yearly operating hours. A larger heat pump does not necessarily mean less OPEX — the integration is crucial.

Fig. 11 presents the total annual OPEX in relation to the CAPEX. Most HO-HPs are in a region of high CAPEX and OPEX. However, the TO-HPs provide smaller CAPEX and especially, OPEX. On the basis of this Figure the difference between NPV TO-HP and IRR TO-HP can be explained. The IRR TO-HP is maximizing the rate of return of the investment. This is reflected by accepting higher OPEX than the NPV TO-HP, but lower CAPEX. Thus, recovering the investment quicker. On the other hand, the NPV TO-HP is maximizing the future value and consequently, a minimum of OPEX is reached. The choice of metric depends on the intentions of the investor. However, with regards to environmental aspects and CO_2 pricing, the NPV TO-HP should be favoured.

Additionally, the effect of the temperature difference $\Delta T_{min,hp}$ has been investigated. The parameter has been varied for the TO-HP optimization with the NPV as the objective value. Fig. 12 emphasizes the importance of the temperature difference $\Delta T_{min,hp}$. The impact on the NPV cannot be understated. The NPV nearly doubles by decreasing the $\Delta T_{min,hp}$ from 12.5 K to 2.5 K. The star marks the $\Delta T_{min,hp}$ value of 6.25 K, which is applied in this study.

The chosen dimensions and results of the techno-economic assessment of the resulting heat pumps is depicted in Table 5. It becomes clear, that neither the largest heat pump nor the heat pump with the highest COP provides the best economic and thermodynamic performance.

The integration of the TAM HP can already provide OPEX savings of 1.75% but has very high CAPEX due to its large heating capacity. With an IRR of 18.4% and an NPV of 167,183 €, it is already a very worthwhile investment.

Table 5
Techno-economic assessment of the resulting heat pumps.

	Without HP	TAM HP	OPEX TO-HP	NPV TO-HP	IRR TO-HP
$\dot{Q}_{sink}$ (kW)	–	347	252	234	122
COP (–)	–	2.56	2.41	2.48	3.17
CAPEX (€)	–	162,925	121,671	113,936	72,893
Operating hours (h)	–	2,180	7491	7545	7556
OPEX (€)	1,824,157	1,792,844	1,754,963	1,755,150	1,772,224
Abs. OPEX savings (€)	–	31,314	69,194	69,007	51,933
Rel. OPEX savings (%)	–	1.75	3.94	3.93	2.93
IRR (%)	–	18.4	56.3	60	70.5
NPV (€)	–	167,183	610,155	615,989	476,556

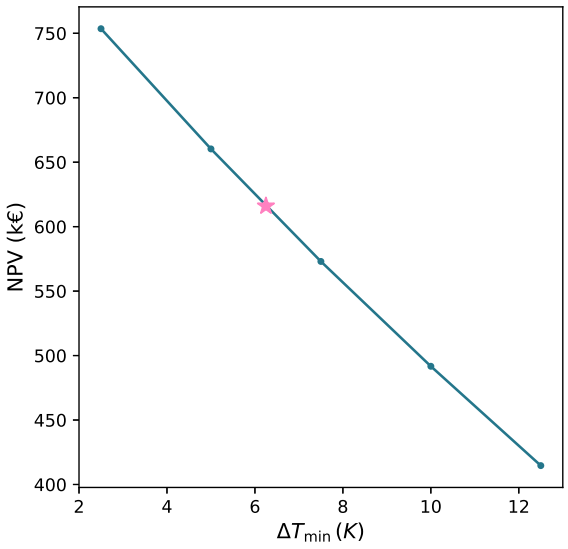

Fig. 12. The impact of $\Delta T_{min,hp}$ on the NPV of the heat pump integration.

The TO-HPs can fully exploit the knowledge of the entire process data and thus determine the optimal parameters. Optimizing solely for the OPEX provides good results with a high number of operating hours. However, to thoroughly optimize the CAPEX need to be considered. The IRR of the NPV TO-HP and IRR TO-HP are very high with 60% and 70.5%, respectively. The previously described discrepancy between the IRR and NPV as optimization objectives is emphasized by the data.

Furthermore, the specific investment cost curves presented in Fig. 4 differ especially in the region of smaller heating capacities. The applied cost estimation provides a lower specific cost in the mentioned region, which leads to the choice of smaller heat pumps. Consequently, the application of a different CAPEX estimation function potentially results in larger heat pumps.

5. Conclusion

The present work compares and demonstrates three approaches to integrate heat pumps into industrial processes with simulated data of the process' operating points. Furthermore, it contributes a new method for dynamic heat pump integration, which selects the optimal design parameters of a heat pump for non-continuous processes. The findings highlight that by utilizing the new methodology, a 33% smaller heat pump with more economic parameters is found, leading to a reduction in annual OPEX by 3.93% compared to the 1.75% OPEX reduction of the TAM HP. The smaller size and greater savings shows particularly in the evaluation of the profitability of the investments. The NPV and IRR have been more than tripled by the optimization. The increase in the heat pump's operating hours is identified as the primary contributing factor to the observed improvements.

The current study includes some assumptions. The present work assumes GCCs with a fixed amount of heat recovery. However, in reality the heat recovery is also subject to process fluctuations. Methods, such as the adapted GCC or the modified energy transfer diagrams could aid this assumption in the future. Furthermore, the applied heat pump model and the feasibility criterion do not consider part load. The heat pumps part load performance is likely to impact the HPs design parameters. Additionally, in the present study only latent heat pumps are considered, but the proposed methodology could also handle the choice of heat pump type for the given process.

The inspiration for future work is plentiful. The methodology will be expanded by part load modelling and heat pump type selection. To explore the flexibility potential further, it would be beneficial to incorporate heat source & sink storages.

CRediT authorship contribution statement

Jasper V.M. Walden: Writing – review & editing, Writing – original draft, Visualization, Validation, Software, Resources, Methodology, Investigation, Formal analysis, Data curation, Conceptualization. **Beat Wellig:** Writing – review & editing, Supervision. **Panagiotis Stathopoulos:** Writing – review & editing, Supervision.

Declaration of competing interest

The authors declare that they have no known competing financial interests or personal relationships that could have appeared to influence the work reported in this paper.

Data availability

Data will be made available on request.

Acknowledgements

The authors declare no competing interests. This research did not receive any specific grant from funding agencies in the public, commercial, or not-for-profit sectors.

References

[1] IEA. World energy outlook 2022. Paris; 2022, http://dx.doi.org/10.1787/3a469970-en, URL https://www.iea.org/reports/world-energy-outlook-2022.
[2] European Commission. An EU strategy on heating and cooling. 2016, URL https://energy.ec.europa.eu/topics/energy-efficiency/heating-and-cooling_en.
[3] Linnhoff B, Flower JR. Synthesis of heat exchanger networks: I. Systematic generation of energy optimal networks. AIChE J 1978;24(4):633–42. http://dx.doi.org/10.1002/aic.690240411.
[4] Klemeš JJ, Kravanja Z. Forty years of heat integration: Pinch analysis (PA) and mathematical programming (MP). Curr Opin Chem Eng 2013;2(4):461–74. http://dx.doi.org/10.1016/j.coche.2013.10.003.
[5] Klemeš JJ, Varbanov PS, Walmsley TG, Jia X. New directions in the implementation of Pinch Methodology (PM). Renew Sustain Energy Rev 2018;98:439–68. http://dx.doi.org/10.1016/j.rser.2018.09.030.
[6] Linnhoff B, Ashton GJ, Obeng ED. Process integration of batch processes. In: IChemE symposium series, vol. 109. 1988, p. 221–37.

[7] Marechal F, Kalitventzeff B. Targeting the integration of multi-period utility systems for site scale process integration. Appl Therm Eng 2003;23(14):1763–84. http://dx.doi.org/10.1016/S1359-4311{%}2803{%}2900142-X.

[8] Varbanov PS, Klemeš JJ. Integration and management of renewables into total sites with variable supply and demand. Comput Chem Eng 2011;35(9):1815–26. http://dx.doi.org/10.1016/j.compchemeng.2011.02.009.

[9] Atkins MJ, Walmsley MR, Neale JR. The challenge of integrating non-continuous processes – milk powder plant case study. J Clean Prod 2010;18(9):927–34. http://dx.doi.org/10.1016/j.jclepro.2009.12.008.

[10] Eiholzer T, Olsen D, Hoffmann S, Sturm B, Wellig B. Integration of a solar thermal system in a medium-sized brewery using pinch analysis: Methodology and case study. Appl Therm Eng 2017;113:1558–68. http://dx.doi.org/10.1016/j.applthermaleng.2016.09.124.

[11] Townsend DW, Linnhoff B. Heat and power networks in process design. Part I: Criteria for placement of heat engines and heat pumps in process networks. AIChE J 1983;29(5):742–8. http://dx.doi.org/10.1002/aic.690290508.

[12] Becker H, Vuillermoz A, Maréchal F. Heat pump integration in a cheese factory. Appl Therm Eng 2012;43:118–27. http://dx.doi.org/10.1016/j.applthermaleng.2011.11.050.

[13] Walmsley TG, Klemes JJ, Walmsley M, Atkins MJ, Varbanov PS. Innovative hybrid heat pump for dryer process integration. Chem Eng Trans 2017;57:1039–44. http://dx.doi.org/10.3303/CET1757174, URL https://www.cetjournal.it/index.php/cet/article/view/CET1757174.

[14] Schlosser F, Arpagaus C, Walmsley TG. Heat pump integration by pinch analysis for industrial applications: A review. Chem Eng Trans 2019;(76):7–12. http://dx.doi.org/10.3303/CET1976002.

[15] Wallerand AS, Kermani M, Kantor I, Maréchal F. Optimal heat pump integration in industrial processes. Appl Energy 2018;219:68–92. http://dx.doi.org/10.1016/j.apenergy.2018.02.114.

[16] Stampfli JA, Atkins MJ, Olsen DG, Walmsley MR, Wellig B. Practical heat pump and storage integration into non-continuous processes: A hybrid approach utilizing insight based and nonlinear programming techniques. Energy 2019;182:236–53. http://dx.doi.org/10.1016/j.energy.2019.05.218.

[17] Agner R, Ong BHY, Stampfli JA, Krummenacher P, Wellig B. A graphical method for combined heat pump and indirect heat recovery integration. Energies 2022;15(8):2829. http://dx.doi.org/10.3390/en15082829.

[18] Seevers J-P, Schlosser F, Peesel RH, Hesselbach J. Dimensioning of heat pump systems based on pinch analysis and energy monitoring data. Chem Eng Trans 2018;70:787–92. http://dx.doi.org/10.3303/CET1870132, URL https://www.cetjournal.it/index.php/cet/article/view/CET1870132.

[19] Becker H, Maréchal F. Targeting industrial heat pump integration in multi-period problems. In: 11th international symposium on process systems engineering. Computer aided chemical engineering, vol. 31, Elsevier; 2012, p. 415–9. http://dx.doi.org/10.1016/B978-0-444-59507-2.50075-5.

[20] Yang M, Li T, Feng X, Wang Y. A simulation-based targeting method for heat pump placements in heat exchanger networks. Energy 2020;203:117907. http://dx.doi.org/10.1016/j.energy.2020.117907.

[21] Lincoln BJ, Kong L, Pineda AM, Walmsley TG. Process integration and electrification for efficient milk evaporation systems. Energy 2022;258:124885. http://dx.doi.org/10.1016/j.energy.2022.124885.

[22] Ghaderi M, Hosseinnia SM, Sorin M. Assessment of waste heat recovery potential in greenhouse ventilation systems using dynamic pinch analysis. Appl Therm Eng 2023;227:120363. http://dx.doi.org/10.1016/j.applthermaleng.2023.120363.

[23] Hosseinnia SM, Sorin M. A systematic pinch approach to integrate stratified thermal energy storage in buildings. Energy Build 2021;232:110663. http://dx.doi.org/10.1016/j.enbuild.2020.110663.

[24] Lal NS, Atkins MJ, Walmsley TG, Walmsley MR, Neale JR. Insightful heat exchanger network retrofit design using Monte Carlo simulation. Energy 2019;181:1129–41. http://dx.doi.org/10.1016/j.energy.2019.06.042.

[25] Schlosser F, Jesper M, Vogelsang J, Walmsley TG, Arpagaus C, Hesselbach J. Large-scale heat pumps: Applications, performance, economic feasibility and industrial integration. Renew Sustain Energy Rev 2020;133:110219. http://dx.doi.org/10.1016/j.rser.2020.110219.

[26] Virtanen P, Gommers R, Oliphant TE, Haberland M, Reddy T, Cournapeau D, et al. SciPy 1.0: Fundamental algorithms for scientific computing in Python. Nature Methods 2020;17:261–72. http://dx.doi.org/10.1038/s41592-019-0686-2.

[27] Storn R, Price K. Differential evolution – A simple and efficient heuristic for global optimization over continuous spaces. J Global Optim 1997;11(4):341–59. http://dx.doi.org/10.1023/A:1008202821328.

[28] Towler G. Chemical engineering design: Principles, practice, and economics of plant and process design. 2nd ed. Oxford and Waltham, MA: Butterworth-Heinemann; 2012, (Online-Ausg.). URL http://site.ebrary.com/lib/alltitles/Doc?id=10562149.

[29] Turton R, Bailie RC, Whiting WB, Shaeiwitz JA, Bhattacharyya D. Analysis, synthesis, and design of chemical processes. Prentice Hall international series in the physical and chemical engineering sciences, 4th ed. Upper Saddle River, N.J. and Munich: Prentice Hall; 2012.

[30] Peters MS, Timmerhaus KD. Plant design and economics for chemical engineers. McGraw-Hill chemical engineering series, 4th ed. New York: McGraw-Hill; 1991.

[31] Lang HJ. Engineering approach to preliminary cost estimates. Chem Eng 1947;54(9):130–3.

[32] Williams R. Six-tenths factor aids in approximating costs. Chem Eng 1947;54(12):124–5.

[33] Pieper H, Ommen T, Buhler F, Paaske BL, Elmegaard B, Markussen WB. Allocation of investment costs for large-scale heat pumps supplying district heating. Energy Procedia 2018;147:358–67. http://dx.doi.org/10.1016/j.egypro.2018.07.104.

[34] Zühlsdorf B, Bühler F, Bantle M, Elmegaard B. Analysis of technologies and potentials for heat pump-based process heat supply above 150 °C. Energy Convers Manag X 2019;2:100011. http://dx.doi.org/10.1016/j.ecmx.2019.100011.

[35] Schlosser F. Integration von Wärmepumpen zur Dekarbonisierung der industriellen Wärmeversorgung. Universität Kassel; 2021, http://dx.doi.org/10.17170/KOBRA-202103023389.

[36] European Commission, Joint Research Centre. Long term (2050) projections of techno-economic performance of large-scale heating and cooling in the EU. Publications Office; 2017, http://dx.doi.org/10.2760/24422.

[37] IEA. Applications of industrial heat pumps. Final report, part 1 and 2. Report No. HPPAN35-1, 2014.

[38] Giampieri A, Ling-Chin J, Ma Z, Smallbone A, Roskilly AP. A review of the current automotive manufacturing practice from an energy perspective. Appl Energy 2020;261:114074. http://dx.doi.org/10.1016/j.apenergy.2019.114074.

[39] Saini P, Ghasemi M, Arpagaus C, Bless F, Bertsch S, Zhang X. Techno-economic comparative analysis of solar thermal collectors and high-temperature heat pumps for industrial steam generation. Energy Convers Manage 2023;277:116623. http://dx.doi.org/10.1016/j.enconman.2022.116623.